

# Photonic crystal slot nanobeam slow light waveguides for refractive index sensing

Bowen Wang,<sup>1,2,a)</sup> Mehmet A. Dündar,<sup>1</sup> Richard Nötzel,<sup>1</sup> Fouad Karouta,<sup>1,b)</sup> Sailing He,<sup>2</sup> and Rob W. van der Heijden<sup>1</sup>

<sup>1</sup>COBRA Research Institute, Eindhoven University of Technology, P.O. Box 513, NL-5600 MB Eindhoven, The Netherlands

<sup>2</sup>Centre for Optical and Electromagnetic Research, KTH-ZJU Joint Research Center of Photonics (JORCEP), Zijingang Campus, Zhejiang University, Hangzhou 310058, China

(Received 2 June 2010; accepted 16 September 2010; published online 11 October 2010)

We present the design, fabrication, and photoluminescence experiment of InGaAsP photonic crystal slot nanobeam slow light waveguides with embedded InAs quantum dots. The strong confinement of electric field in the slot region is confirmed by the measured record high sensitivity of  $7 \times 10^2$  nm per refractive index unit (RIU) to the refractive index change of the environment. A cavity, formed by locally deflecting the two beams toward each other, gives an even higher sensitivity of about  $9 \times 10^2$  nm/RIU. © 2010 American Institute of Physics.

[doi:10.1063/1.3497296]

Optofluidics, referring to a class of optical systems that are synthesized with fluids, is an emerging technology for synthetic/analytical chemistry and nanobiotechnology. Here, light is used for controlling and efficiently analyzing fluids, colloidal solutions, solids in a fluid, etc, in microscale devices.<sup>1,2</sup> Sensors are among the fundamental elements of optofluidics. Miniaturization of label-free optical sensors is of particular interest for realizing ultracompact lab-on-a-chip applications with dense arrays of functionalized spots for multiplexed sensing, that may lead to portable, low cost and low power devices. Many efforts exist to realize small devices and among them are photonic crystals (PhCs). So far, many kinds of PhC sensors relying on regular PhCs, PhC waveguides and PhC cavities have been demonstrated.<sup>3–10</sup>

Recently there has been much interest in cavities realized in free standing nanobeams patterned with a one-dimensional lattice of holes.<sup>11–16</sup> Single nanobeams are studied for their exceptional high quality ( $Q$ ) factor and small modal volume.<sup>11,12</sup> Coupled nanobeams with air slot are invented to tune the modes<sup>13–15</sup> and achieve an optomechanical cavity.<sup>16</sup> These structures were made in passive dielectrics as Si,<sup>11,13–15</sup> SiO<sub>2</sub> (Ref. 12) or SiN.<sup>16</sup> Very recently, single nanobeams made in III-V semiconductors are fabricated to achieve lasing.<sup>17,18</sup> In all these structures, the cavities are made by changing the lattice constant, or by modifying the radius of the holes and the distance between the holes. In addition, because of the strong optical fields that exists in the slot region,<sup>8,19</sup> these devices are proposed to have applications in sensing. However, no experiment about sensing based on these structures has been reported until now.

In this work, we investigate InGaAsP PhC slot nanobeam slow light waveguides with embedded InAs quantum dots (QDs) consisting of two parallel suspended beams separated by a small gap, each patterned with a one-dimensional (1D) line of holes. Such a structure exhibits a resonance near its band edge frequency where the group velocity is near

zero. No modification is made to form a local cavity. By measuring the resonant wavelength for different analytes, we report a high sensitivity  $S = \Delta\lambda / \Delta n$  of  $7 \times 10^2$  nm per refractive index unit (RIU). For another structure with a cavity, a sensitivity of  $9 \times 10^2$  nm/RIU is measured. These record high values for  $S$  correspond directly to the large overlap of the mode field with the analyte,<sup>10</sup> particularly in the slot region. This kind of structure based on luminescent III-V semiconductors is attractive as it offers the full on-chip integration with sources, or the operation as lasers to increase the refractive index resolution.<sup>4</sup> In addition, it can be employed using remote readout, not requiring the delicate attachment of optical fibers or electrical wiring.

A PhC slot nanobeam slow light waveguide was designed by using MIT photonic bands software package (MPB) (Ref. 20) and three-dimensional finite-difference time-domain method.<sup>21</sup> The top view and cross sectional view of the unit cell of waveguide used in the bandstructure calculation is shown in Figs. 1(a) and 1(b), respectively. The waveguide is defined by the lattice constant (490 nm), width of

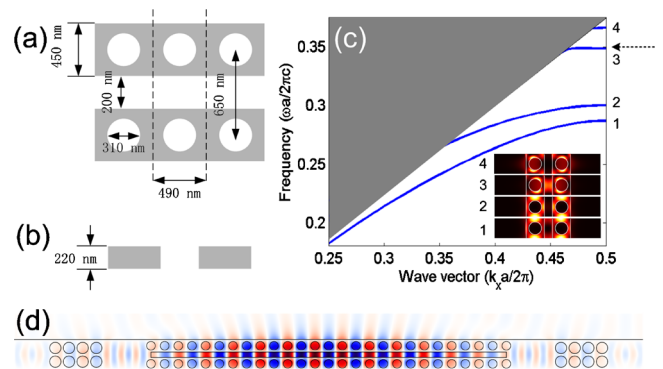


FIG. 1. (Color online) Schematic sketch of a PhC slot nanobeam slow light waveguide from (a) top view, (b) cross-sectional view. A unit cell is marked by two dashed lines. (c) Band structure of the waveguide. The gray region is the light cone of water. The inset shows the intensity distributions of four band-edge modes in the central plane from bottom to top accordingly. (d) The electrical field ( $E_y$ ) profile of the slot mode of a finite waveguide with some extra mirrors infiltrated with distilled water in the central plane.

<sup>a)</sup>Electronic mail: wang.bowen@tue.nl.

<sup>b)</sup>Present address: Research School of Physics & Engineering, Australian National University, Canberra, Australia.

single nanobeam (450 nm), width of the slot area (200 nm), distance between the symmetric holes (650 nm), diameter of the holes (310 nm) and the thickness of the membrane (220 nm). Since the nanobeam is intended as a liquid sensor, the bandstructure calculation from MPB is performed for an environment refractive index of 1.333, corresponding to water, and is displayed in Fig. 1(c). There are four bands under the light cone of water, whose cutoff wavelengths are at 1706.8 nm ( $\omega a/2\pi c=0.2871$ ), 1631.5 nm ( $\omega a/2\pi c=0.3003$ ), 1404.7 nm ( $\omega a/2\pi c=0.3488$ ), and 1336.9 nm ( $\omega a/2\pi c=0.3665$ ), respectively. The intensity distributions of four band-edge modes in the central plane of the unit cell are shown in the inset of Fig. 1(c). For the band-edge mode of the third band, the light is strongly localized inside the slot region and holes. We will call it slot mode later. The slot mode profile of this waveguide is similar to the even mode profile around cavities in coupled nanobeams as described in Refs. 13–15 but is not the same, which will be discussed later. For a real sample, the length of waveguides is always finite. Additionally there is a constraint on the length of these waveguides because they need to be able to support their own weight and survive in the fabrication and processing. A PhC slot nanobeam slow light waveguide with 27 periods was designed. In our simulation, the slot modes of the cavity infiltrated with distilled water ( $n=1.333$ ) and sugar/water solution ( $n=1.3417$ ) are at 1416.5 nm and 1422.8 nm respectively, with  $Q$  factors of 2000. Because the structure is finite, losses occur near the two ends. To decrease these losses, additional PhC mirrors with lattice constant of 490 nm and hole diameter of 400 nm were added, which increased the calculated  $Q$  factors to 3000. The electrical field ( $E_y$ ) profile of the slot mode of the finite waveguide with the extra mirrors infiltrated with distilled water in the central plane is presented in Fig. 1(d). The light is strongly localized in the central part of PhC slot nanobeam slow light waveguide. The light localization of the band edge mode in the central part of our 1D finite length waveguide is analogous to the light localization of band edge modes in finite two dimensional PhCs in Ref. 22. By relating the peak position change with the change of refractive index, we obtain an impressive sensitivity value of 724 nm/RIU. Comparing with the even mode in the coupled nanobeams cavity [cf. Fig. 2 in Ref. 14] where the light is localized in the slot region but also in the semiconductor, our slot mode has more light confined in the low refractive index region, i.e., in the slot region but also in the holes.

An InGaAsP PhC slot nanobeam slow light waveguide was fabricated on a 220 nm thick InGaAsP membrane which contains a single layer of self-assembled InAs QDs (density  $3 \times 10^{10} \text{ cm}^{-2}$ ).<sup>23</sup> The details about the fabrication process can be found in Ref. 10. Figure 2(a) shows the scanning electron microscope (SEM) image of the InGaAsP slot PhC nanobeam slow light waveguide with the designed parameters. Analyte was placed on the top of the sample from a pipette. This entirely immerses the nanobeam structure with the liquid. Then a 0.15 mm thick cover glass was placed on the filled sample in order to avoid water evaporation and to achieve a flat and constant thickness layer of analyte on top of the sample. Since excess fluid is present, not only the holes, but also the top of the sample and under-etched void is filled with the liquid. Because of the incorporated QDs, a photoluminescence (PL) experiment can be conducted easily

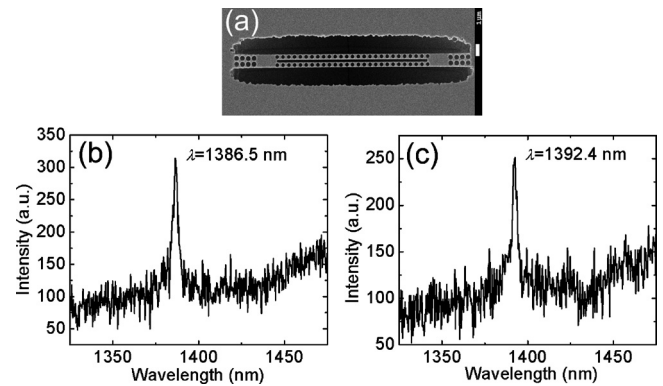


FIG. 2. (a) SEM image of an InGaAsP PhC slot nanobeam slow light waveguide; PL spectrum of the waveguide with the infiltration of (b) distilled water ( $n=1.333$ ), (c) sugar/water solution ( $n=1.342$ ).

by using a continuous wave CW diode laser ( $\lambda=660 \text{ nm}$ ) as an excitation source. An optical microscope objective with numerical aperture (NA)=0.5 and magnification of 50 is used for both excitation of the cavities and collection of the PL. After dispersing the PL in a 50 cm focal length monochromator, the collected signal is detected by a liquid nitrogen cooled InGaAs camera.

To measure the sensitivity of our structure, the sample was infiltrated with distilled water and sugar/water solution separately with known refractive indices.<sup>24</sup> The refractive indices of distilled water and sugar/water solution are 1.333 and 1.342, respectively. Figure 2(b) shows the PL spectrum of the InGaAsP slot PhC nanobeam slow light waveguide with the infiltration of distilled water. The peak at 1386.5 nm is the slot mode, with a  $Q$  factor of 500. Figure 2(c) shows the PL spectrum of the same waveguide with the infiltration of sugar/water solution. The peak redshifts to 1392.4 nm. This gives a sensitivity of  $7 \times 10^2 \text{ nm/RIU}$ , which has been confirmed several times later. A sensitivity close to the predicted value of 724 nm/RIU, implies that the calculated mode pattern agrees with experiment. Previously the high intensity in a different slot structure was measured by locally probing the electromagnetic (EM) field distribution by a scanning near-field optical microscopy experiment.<sup>13</sup> In the present work we probe it directly by a sensitivity experiment as previously demonstrated.<sup>10</sup> The structure is promising for application after improving the  $Q$  factor, while the  $Q$  factor can be improved by introducing a better mirror just on the ends of the slot region.<sup>22</sup> The slight discrepancy between simulation and experiment of the peak position,  $Q$  factor and sensitivity can be attributed to several effects, including the uncertainty of the membrane thickness after an  $\text{O}_2$  plasma and  $\text{H}_3\text{PO}_4$  etch, and the roughness in the slot region which weakens the localization of the light inside the slot region.

Because of the over etching of one device caused change in device geometry, we also have an InGaAsP PhC slot nanobeam slow light waveguide with stuck nanobeams, which is shown in Fig. 3(a). In this device, the parameters are the same as those we mention above, except for the hole diameter, which is increased to 330 nm. However, for this waveguide, the nanobeams bend inward which makes the slot region narrow in the central part and a cavity is formed. The bend may be due to the weak wall because of the larger hole diameter. We measure the sensitivity of this structure in the same way used before. Figure 3(b) shows the PL spectrum of

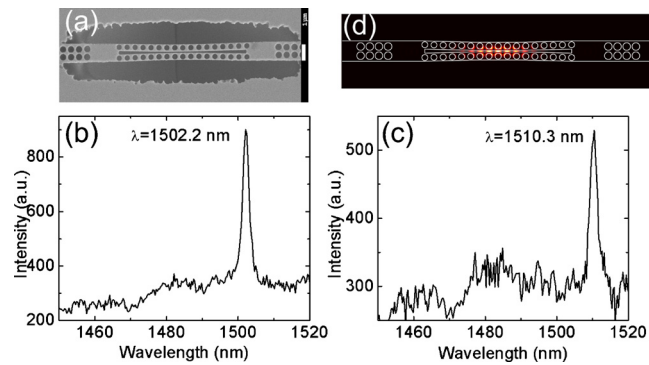


FIG. 3. (Color online) (a) SEM image of a cavity type InGaAsP PhC slot nanobeam slow light waveguide; PL spectrum of the cavity type waveguide with the infiltration of (b) distilled water ( $n=1.333$ ), (c) sugar/water solution ( $n=1.342$ ); (d) The field intensity distribution for the slot mode of the cavity type waveguide infiltrated with distilled water in the central plane.

the cavity with the infiltration of distilled water. The peak at 1502.2 nm is the slot cavity mode, with a  $Q$  factor of 700. Figure 3(c) shows the PL spectrum of the same structure with the infiltration of sugar/water solution. The peak redshifts to 1510.3 nm. This gives a sensitivity of about  $9 \times 10^2$  nm/RIU. Compared to the normal waveguide, the resonant wavelength shows a redshift of 100 nm, while this cavity has a higher sensitivity and a higher  $Q$  factor. The redshift in the resonant wavelength is due to the decrease in the separation between the two nanobeams.<sup>14,15</sup> We have also modeled the bend case in our simulation, and found that the slot modes of the cavity infiltrated with distilled water ( $n=1.333$ ) and sugar/water solution ( $n=1.3417$ ) are at 1477.0 nm and 1482.6 nm respectively, which gives a sensitivity of 643 nm/RIU. The intensity distribution of the slot mode of the cavity type waveguide infiltrated with distilled water in the central plane is presented in Fig. 3(d). The light is still strongly localized in the slot region. The difference between the experiment and simulation results is caused by parameters uncertainty as inferred from SEM image. The higher sensitivity in the experiment may be also caused by the larger hole size in the bend structure.

In conclusion, we presented the sensitivity to the refractive index changes of the analyte of InGaAsP PhC slot nanobeam slow light waveguides as a measure of the intensity distribution in the low index region, particularly the slot region. We report a high sensitivity of  $7 \times 10^2$  nm/RIU and for a normal structure and a higher sensitivity of  $9 \times 10^2$  nm/RIU for a cavity type structure. By introducing a real cavity into the waveguide, we believe that the  $Q$  factor could be increased by a few orders of magnitude<sup>14,16</sup> and a

very high refractive index resolution could be achieved. Such a high  $Q$  PhC sensor was realized recently with a 2D PhC air slot cavity.<sup>25</sup>

B. Wang thanks Dr. Yaocheng Shi for useful discussion. The authors acknowledge the support from the BrainBridge project (ZJU-TU/e and Philips Research collaboration), AOARD, and the National Natural Science Foundation of China (Grant No. 60907018).

- <sup>1</sup>D. Psaltis, S. R. Quake, and C. Yang, *Nature (London)* **442**, 381 (2006).
- <sup>2</sup>C. Monat, P. Domachuk, and B. J. Eggleton, *Nat. Photonics* **1**, 106 (2007).
- <sup>3</sup>J. Topol'ančič, P. Bhattacharya, J. Sabarinathan, and P.-C. Yu, *Appl. Phys. Lett.* **82**, 1143 (2003).
- <sup>4</sup>S. Kita, K. Nozaki, and T. Baba, *Opt. Express* **16**, 8174 (2008).
- <sup>5</sup>J. Wu, D. Day, and M. Gu, *Appl. Phys. Lett.* **92**, 071108 (2008).
- <sup>6</sup>D. F. Dorfner, T. Hürlimann, T. Zabel, L. H. Frandsen, G. Abstreiter, and J. J. Finley, *Appl. Phys. Lett.* **93**, 181103 (2008).
- <sup>7</sup>P. S. Nunes, N. A. Mortensen, J. P. Kutter, and K. B. Mogensen, *Opt. Lett.* **33**, 1623 (2008).
- <sup>8</sup>A. Di Falco, L. O'Faolain, and T. F. Krauss, *Appl. Phys. Lett.* **94**, 063503 (2009).
- <sup>9</sup>S. Kim, J. Lee, H. Jeon, and H. J. Kim, *Appl. Phys. Lett.* **94**, 133503 (2009).
- <sup>10</sup>M. A. Dündar, E. C. I. Ryckebosch, R. Nötzel, F. Karouta, L. J. van IJendoorn, and R. W. van der Heijden, *Opt. Express* **18**, 4049 (2010).
- <sup>11</sup>P. B. Deotare, M. W. McCutcheon, I. W. Frank, M. Khan, and M. Lončar, *Appl. Phys. Lett.* **94**, 121106 (2009).
- <sup>12</sup>Y. Gong and J. Vučković, *Appl. Phys. Lett.* **96**, 031107 (2010).
- <sup>13</sup>K. Foubert, L. Lalouat, B. Cluzel, E. Picard, D. Peyrade, F. de Fornel, and E. Hadji, *Appl. Phys. Lett.* **94**, 251111 (2009).
- <sup>14</sup>P. B. Deotare, M. W. McCutcheon, I. W. Frank, M. Khan, and M. Lončar, *Appl. Phys. Lett.* **95**, 031102 (2009).
- <sup>15</sup>I. W. Frank, P. B. Deotare, M. W. McCutcheon, and M. Lončar, *Opt. Express* **18**, 8705 (2010).
- <sup>16</sup>M. Eichenfield, R. Camacho, J. Chan, K. J. Vahala, and O. Painter, *Nature (London)* **459**, 550 (2009).
- <sup>17</sup>Y. Zhang, M. Khan, Y. Huang, J. Ryou, P. Deotare, R. Dupuis, and M. Lončar, *Appl. Phys. Lett.* **97**, 051104 (2010).
- <sup>18</sup>Y. Gong, B. Ellis, G. Shambat, T. Sarmiento, J. S. Harris, and J. Vučković, *Opt. Express* **18**, 8781 (2010).
- <sup>19</sup>V. R. Almeida, Q. Xu, C. A. Barrios, and M. Lipson, *Opt. Lett.* **29**, 1209 (2004).
- <sup>20</sup>S. G. Johnson and J. D. Joannopoulos, *Opt. Express* **8**, 173 (2001).
- <sup>21</sup>A. F. Oskooi, D. Roundy, M. Ibanescu, P. Bermel, J. D. Joannopoulos, and S. G. Johnson, *Comput. Phys. Commun.* **181**, 687 (2010).
- <sup>22</sup>L. Ferrier, P. Rojo-Romeo, E. Drouard, X. Letatre, and P. Viktorovitch, *Opt. Express* **16**, 3136 (2008).
- <sup>23</sup>R. Nötzel, S. Anantathanasarn, R. P. J. van Veldhoven, F. W. M. van Otten, T. J. Eijkemans, A. Trampert, B. Satpati, Y. Barbarin, E. A. J. M. Bente, Y. S. Oei, T. de Vries, E. J. Geluk, B. Smalbrugge, M. K. Smit, and J. H. Wolter, *Jpn. J. Appl. Phys., Part 1* **45**, 6544 (2006).
- <sup>24</sup>F. Schneider, *Sugar Analysis-ICUMSA*, [International Commission for Uniform Methods of Sugar Analysis, (ICUMSA), 1979, (ICUMSA), 2009].
- <sup>25</sup>J. Jágerská, H. Zhang, Z. Diao, N. L. Thomas, and R. Houdré, *Opt. Lett.* **35**, 2523 (2010).